

## Biological Effect of Cobalt Oxide Nanoparticles Synthesized from (*Cinnamon* and *Nigella sativa*) Extracts and Chemical Method: A Comparative Study

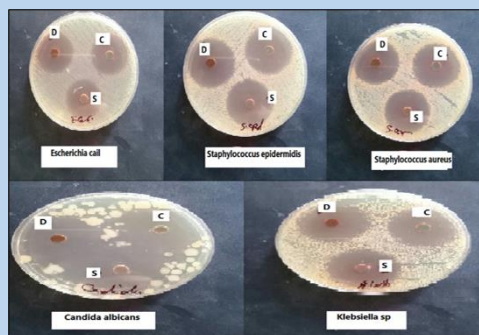
Ghasaq Z. Alwan<sup>1,\*</sup>, Emtinan Mohammed Jawad<sup>1,2</sup>, Hana H. Kareem<sup>1,3</sup> & Raed Jumah Almansouri<sup>4</sup>

(Type: Full Article). Received 24<sup>th</sup> May 2025, Accepted 15<sup>th</sup> Jul. 2025, Published: 1<sup>st</sup> Mar. 2026,

DOI: <https://doi.org/10.35552/anjur.a.39.3.2540>

(This article belongs to the Special Issue: Sustainable Materials and Chemistry for Energy and Environmental Applications)

**Abstract:** This study involved the synthesis of cobalt oxide (Co<sub>3</sub>O<sub>4</sub>) nanoparticles (NPs). Using a sustainable green utilization of *Cinnamon* (*Cinnamomum zeylanicum*) and *Nigella sativa* extracts, alongside a conventional chemical synthesis method for comparison. Comprehensive structural, morphological, and optical characterizations confirmed the successful synthesis of Co<sub>3</sub>O<sub>4</sub> NPs with distinct properties. XRD analysis revealed smaller crystalline sizes for green-synthesized NPs (5.49 nm for *Cinnamon* and 7.22 nm for *Nigella sativa*) compared to chemically synthesized ones (10.6 nm), while FTIR identified functional groups contributing to enhanced chemical and biological activity. FESEM and AFM analyses showed improved surface topography, reduced roughness, and higher effective surface areas in biogenically NPs. UV-visible spectroscopy demonstrated enhanced electronic properties, with band gaps of 1.61 eV and 1.59 eV for *Cinnamon* and *Nigella sativa*-derived NPs, respectively, as compared to 1.43 eV for chemically synthesized NPs. Biological assays revealed superior antimicrobial activity of green-synthesized NPs, particularly *Cinnamon*-derived NPs against *Staphylococcus aureus* (34 mm), *Escherichia coli* (30 mm), and *Nigella sativa*-derived NPs against *Candida albicans* (41 mm). The synergistic action between plant-derived compounds such as Cinnamaldehyde and Thymoquinone and cobalt oxide nanoparticles enhanced their antimicrobial efficacy. In conclusion, the use of plant extracts for synthesizing Co<sub>3</sub>O<sub>4</sub> NPs offers a sustainable, economical substitute for the chemical approach, producing nanoparticles.



**Keywords:** Antibacterial activity, *Cinnamon*, Co<sub>3</sub>O<sub>4</sub> Nps, green synthesis, Plant extract.

### Introduction

The creation and utilization of metal and metal oxide nanoparticles have attracted considerable interest because of their unique characteristics, which result from their structural features, size, shape, and overall dimensions [1]. These nanoparticles have intrigued researchers for over a century, playing a crucial role across numerous scientific and industrial domains. Transition metal oxides at the nanoscale are particularly noteworthy as a class of materials with diverse applications, including their roles as catalysts, electrodes, semiconductors, sensors, components in solar cells, and ceramic materials, among others [2-4].

The proliferation of antibiotic-resistant bacterial strains exacerbates a major risk to public health by the widespread appearance of infectious illnesses. Antibiotics have been the main line of defense against infections for many years in both community and *medical* settings [5, 6]. However, advancements in nanobiotechnology, especially the tailored synthesis of metal oxide nanomaterials with specific morphologies, exhibit potential for the evolution of new antibacterial substances. Nanoparticles,

in particular, have generated significant attention due to their functional characteristics, which are heavily impacted due to their dimensions and large surface area relative to volume [7, 8]. The utilization of inorganic materials offers distinct advantages, including chemical stability, safety, and biocompatibility [9]. A growing body of literature highlights the antibacterial efficacy of metal oxide nanoparticles, emphasizing their high potential in combating bacterial infections [10] and the chain reactions [11]. The potency of antioxidants is strongly influenced by their concentration and the chemical states of the antioxidants with which they interact [12]. Various antioxidants have been identified as essential for scavenging toxic free radicals in biological systems, mitigating the oxidative stress generated during these processes [13, 14]. Due to their high surface-to-volume ratio, nanostructured materials are anticipated to outperform bulk materials as free radical scavengers, offering enhanced protective capabilities. Nanoparticles' antimicrobial properties also hinge on the structural characteristics of the target organisms. Gram-positive bacteria are typically more resistant to antibacterial treatments than Gram-negative bacteria because of their thicker cell walls. Nanoparticles have

<sup>1</sup> Department of Physics, College of Science, Mustansiriyah University, Baghdad, Iraq.

\* Corresponding author email: ghasaqz.alwan@uomustansiriyah.edu.iq

<sup>2</sup> E-mail: imtenanmj@uomustansiriyah.edu.iq

<sup>3</sup> E-mail: hanakr2007@uomustansiriyah.edu.iq

<sup>4</sup> Directorate of education of Al-Rasafa, Ministry of Education, Baghdad, Iraq. raedpcms@gmail.com

demonstrated encouraging antibacterial properties despite this. When nanoparticles interact with bacterial cells, they damage the integrity of the membrane, resulting in holes and pits that weaken the cell's structure. This interference suppresses respiratory chain enzymes, prevents DNA replication, and eventually results in cell death [15-17]. Several chemical agents, like hydrazine, sodium borohydride, aldehydes, and citrates, as well as radiation sources and functional polymers that operate as reducing agents, are typically used in the traditional synthesis of nanoparticles. Nevertheless, these approaches have a large impact on the environment, are expensive, and use a lot of energy and resources [18, 19]. Recent studies have turned to plant extracts as a sustainable and eco-friendly substitute for nanoparticle manufacturing in response to these issues. In addition to being less harmful, plant-based techniques are safer for human use [2, 20]. Numerous biochemicals found in botanical extracts, including proteins, amino acids, terpenoids, alkaloids, phenolics, and aldehydes, stabilize and enhance the conversion of metal ions into nanostructures. These extracts have negligible contamination risks, are easily handled, and are suitable for industrial synthesis scaling up. Numerous studies have revealed the successful formation of nanoscale metal particles using a range of plant extracts [21, 22]. Achieving exact control over the nanoparticles' size and structure through reaction condition tweaking is a crucial difficulty in their production. Metabolites in plant extracts also serve as capping agents during synthesis, preventing nanoparticle aggregation [23-25]. Since various plant extracts contain multiple amounts and configurations of chemical substances, the features of the created nanoparticles are set by the plant sources [26]. For the manufacturing of  $\text{Co}_3\text{O}_4$  NPs, *cinnamon* (*Cinnamomum zeylanicum*) was used as the plant source in this investigation. *Cinnamon* is widely used as a seasoning agent and in herbal remedies to treat digestive ailments such as diarrhea. Its extract contains a high concentration of bioactive molecules such as cinnamaldehyde, eugenol, and linalool, which exhibit potent antioxidant activity [27]. Additionally, *Nigella sativa*, an herbaceous seasonal plant from the Ranunculaceae family, was also employed for  $\text{Co}_3\text{O}_4$  NP biosynthesis [28]. Cobalt oxides, comprising cobaltous oxide ( $\text{CoO}$ ), cobaltic oxide ( $\text{Co}_2\text{O}_3$ ), and cobaltous oxide ( $\text{Co}_3\text{O}_4$ ), possess unique physicochemical properties that support a wide range of industrial applications [29]. Among these,  $\text{Co}_3\text{O}_4$  has achieved particular care due to its distinctive morphology and redox properties, as well as its nonstoichiometric polymorphic nature [30]. Several studies have investigated biogenic synthesis using plant extracts of cobalt oxide nanoparticles. Dubey *et al.* [31] synthesized cobalt oxide NPs using latex from *Calotropis procera*, while Bibi *et al.* [32] employed *Punica granatum* peel extract for cobalt oxide fabrication. Similarly, Akhlaghi *et al.* [33] used *Trigonella foenum-graecum* (*fenugreek*) leaf extract, and Saeed *et al.* [34] utilized root extracts from *Ziziphus oxyphylla* Edgew.. Alaghemand *et al.* [28] fabricated silver nanoparticles by *Nigella sativa* L. extract, while Anjum *et al.* [35] presented the findings on formation of cobalt oxide NPs using *Cinnamomum zeylanicum*. The purpose of this study is to develop a rapid and efficient method for synthesizing  $\text{Co}_3\text{O}_4$  nanoparticles using plant extracts from *Cinnamomum zeylanicum* and *Nigella sativa* L., alongside a comparative chemical synthesis approach without plant extracts. The study further evaluates the inhibition of these NPs on bacterial and fungal pathogens.

## Materials and Methods

### Materials

Cobalt nitrate  $\text{Co}(\text{NO}_3)_2$ , M.W. 182.92 g/mol was obtained from Alpha Chemika (India). Sodium hydroxide (NaOH, M.W. 40

g/mol), as well as *cinnamon* bark and *Nigella sativa* seeds, were procured from local markets.

### Preparation of $\text{Co}_3\text{O}_4$ NPs with *Nigella sativa* extract

Two grams of *Nigella sativa* seeds were ground using an electric grinder for ten minutes and sieved through a 58-micron mesh. The synthesized powder was mixed into 100 mL of deionized water and then stirred on a magnetic mixer at  $50^\circ\text{C}$  for 30 minutes, yielding a light yellow, transparent solution. Upon cooling to room temperature, the extract was strained four times using Whatman filter paper no. 0.5 separately, 9.15 g of cobalt nitrate was dissolved in 100 mL of deionized water (0.5 M) and stirred on a magnetic mixer at  $50^\circ\text{C}$  till a transparent dark red solution was obtained. Then, 35 mL of the *Nigella sativa* extract was poured in drops into the cobalt nitrate solution, being stirred continuously, culminating in the creation of a reddish-brown aqueous solution. As shown in Fig. (1-A).

### Preparation of $\text{Co}_3\text{O}_4$ NPs with Cinnamon extract

Two grams of *cinnamon* were ground using an electric grinder for ten minutes, next sieved via a 58-micron mesh. The formed powder was mixed into 100 mL of deionized water and then stirred on a magnetic mixer at a temperature of  $50^\circ\text{C}$  for 30 minutes, producing a yellow solution. After reaching room temperature, the extract was strained four times using Whatman filter paper no. 0.5 separately, 9.15 g of cobalt nitrate was dissolved in 100 mL of deionized water (0.5 M) and stirred on a magnetic mixer at  $50^\circ\text{C}$  till a clear ruby-red solution was obtained. Thereafter, 35 mL of the plant extract was poured in drops into the cobalt nitrate solution, being stirred continuously. The mixture was distilled until the solution's color changed to reddish-brown. As illustrated in Fig. (1-B).

### Preparation of $\text{Co}_3\text{O}_4$ NPs by chemical method without using any plant extracts

A total of 9.1 g of cobalt nitrate ( $\text{Co}(\text{NO}_3)_2$ ) was mixed in 100 mL of deionized water and stirred on a magnetic mixer at  $50^\circ\text{C}$  for 30 minutes, producing a red solution upon complete dissolution. In a separate preparation, 4 g of sodium hydroxide (NaOH) was mixed in 100 mL of deionized water to create a 1 M solution and stirred magnetically at  $50^\circ\text{C}$  until fully dissolved. The NaOH solution was then added gradually and dropwise to the cobalt nitrate solution at a steady rate. A distinct color change was observed, with the solution stabilizing to a blackish-blue hue after the addition of 20 mL of the NaOH solution. As shown in Fig.(1-C).

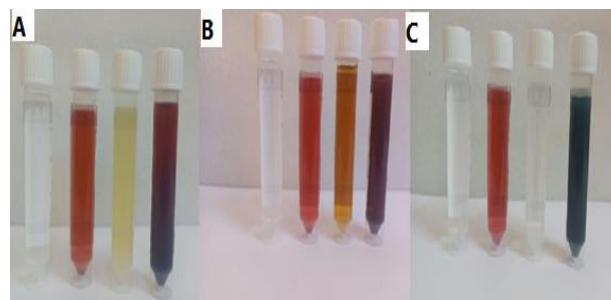


**Figure (1):**  $\text{Co}_3\text{O}_4$  NPs formation steps : (A) using *Nigella sativa* extract. (B) using *Cinnamon* extract (C) using chemical method without using any plant extracts.

### Antimicrobial Activity Measurement

The antimicrobial effect of cobalt oxide nanoparticles ( $\text{Co}_3\text{O}_4$  NPs) synthesized chemically, combined with *cinnamon* and *Nigella sativa* extracts, was evaluated under aerobic conditions with efficient agar diffusion in well plates against various pathogens. The effectiveness of the samples in inhibiting bacterial growth, fungi, and yeast was tested against *Staphylococcus aureus*, *Staphylococcus epidermis*, *Escherichia*

*coli*, *Klebsiella sp.*, and *Candida albicans*. Nutrient agar plates were prepared and inoculated with the test organisms, which were evenly spread using a glass spreader. Agar wells measuring 6 mm in diameter were created in the Muller–Hinton substrate, and 100  $\mu$ L of each test sample, including  $\text{Co}_3\text{O}_4$  NPs, *cinnamon* extract, and *Nigella sativa* extract, were introduced. The plates were incubated under optimal conditions, with fungal and bacterial samples that were cultured for 72 hours at 30 °C and for 24 hours at 37 °C, respectively. The range of the zone of inhibition (ZOI) was calculated with a millimeter scale to determine the antibacterial activity. This technique allowed the diffusion of the test substances into the agar, effectively inhibiting the growth of the test organisms. The experiment was conducted in the Life Sciences Department Laboratory at Mustansiriyah University, demonstrating the potential of these materials as antimicrobial agents.

### Characterization

The characterization of the as-prepared  $\text{Co}_3\text{O}_4$  nanoparticles (NPs) was conducted using various analytical techniques. UV–visible spectrophotometry was performed with a DU-8800D spectrophotometer (China) within the wavelength range of 190–1100 nm. FTIR spectra were recorded using an attenuated total reflection Fourier-transform infrared spectrophotometer (ATR-FTIR, ALPHA - BRUKER). The morphological properties of the  $\text{Co}_3\text{O}_4$  NPs were examined using Field Emission Scanning Electron Microscopy (FESEM, MIRA3 TESCAN). X-ray diffraction (XRD) patterns were recorded with a SHIMADZU XRD-6000 instrument (Japan) employing  $\text{CuK}\alpha$  radiation ( $\lambda = 1.5406 \text{ \AA}$ ). Atomic Force Microscopy (AFM) images were acquired using a Digital Instruments system (Nanoscope III and Dimension 3100).

## Results and Discussion

### XRD Analysis

As seen in Fig. 2, the XRD patterns for  $\text{Co}_3\text{O}_4$  nanoparticles (NPs) were prepared using *Cinnamon* extract, *Nigella sativa* extract, and the chemical method without plant extracts. Several distinct peaks were observed in all patterns for  $\text{Co}_3\text{O}_4$  at  $2\theta = 18.9^\circ, 29.5^\circ, 31.5^\circ, 36.9^\circ, 44.7^\circ, 59.3^\circ,$  and  $65.2^\circ$ , corresponding to the (111), (210), (220), (311), (400), (511), and (440) planes, respectively. These peaks are characteristic of the spinel-type

cubic phase of  $\text{Co}_3\text{O}_4$  (JCPDS Card No. 01-080-1535) [36]. The  $\text{Co}_3\text{O}_4$  NPs prepared with plant extracts exhibited similar peaks, with slight shifts due to lattice strains. Interestingly, a peak at  $2\theta = 15.1^\circ$ , corresponding to the (101) plane, appeared only in the chemically synthesized  $\text{Co}_3\text{O}_4$  NPs [37, 38]. This absence in the plant-assisted samples is attributed to the interaction of organic compounds and other materials present in plant extracts with cobalt during synthesis, which impacts the atomic structure, resulting in a partially amorphous phase [38, 39]. Additionally, the small size of the plant-assisted NPs may contribute to peak broadening in the XRD patterns, causing certain peaks to weaken or disappear at specific angles [37]. The intensity of the peaks for plant-assisted NPs was lower compared to those prepared by the chemical method, indicating reduced crystallinity. The crystallite size of  $\text{Co}_3\text{O}_4$  NPs was computed using the Debye-Scherrer formula,  $D=0.94\lambda/\beta\cos\theta$ , where  $\lambda$  is the wavelength of x-ray (1.5406 Å) for  $\text{CuK}\alpha$  radiation,  $\beta$  is the full width at half maximum and  $\theta$  is the peak position [40]. The average crystallite size was determined to be 5.49 nm for *Cinnamon* extract-assisted NPs, 7.225 nm for *Nigella sativa* extract-assisted NPs, and 10.6 nm for chemically synthesized NPs [41]. Table 1 summarizes XRD characterization and computation of Various Parameters for biogenic  $\text{Co}_3\text{O}_4$  NPs.

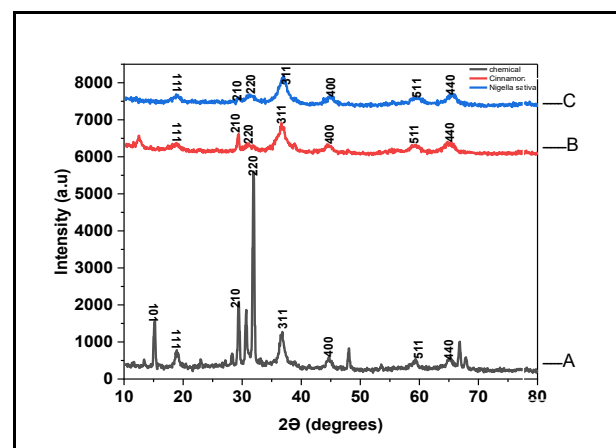


**Figure (2):** X-ray diffraction patterns of  $\text{Co}_3\text{O}_4$  NPs with by (A) chemical method, (B) *Cinnamon* extracts, (c) *Nigella sativa* extract.

**Table (1):** XRD Analysis and calculation of various parameters for  $\text{Co}_3\text{O}_4$  NPs using chemical method

Sr No.	$2\theta$ (Deg.)	FWHM (Deg.)	FWHM (radians.)	dhkl.(Å)	hkl	D (nm)	For unit cell edges: $a = b = c$ (Å)
1	31.8000	0.5000	0.0085	2.8117	220	16.5	7.952
2	36.8440	1.7000	0.0289	2.4376	311	4.9	
3	29.3700	0.5500	0.00935	3.0386	210	14.9	
4	44.6000	1.4000	0.02436	2.0300	400	6.1	
5	15.25	0.62	0.0154	5.8243	101	12.9	
6	18.92	0.68	0.01156	4.6867	111	11.8	
7	59.37	1.48	0.0256	1.5554	511	6.2	
8	65.2	1.77	0.03009	2.0300	400	4.9	

### Analysis using FT-IR

The FT-IR spectral range was maintained between 400 and 4000  $\text{cm}^{-1}$ . The FT-IR spectra of the biosynthesized  $\text{Co}_3\text{O}_4$  nanoparticles. Shown in Fig. 3, provides insight into the various vibrational modes present. A prominent peak observed at 3431  $\text{cm}^{-1}$  is attributed to O–H stretching [42]. Additionally, a slightly elevated peak at 2066  $\text{cm}^{-1}$  corresponds with C–H stretching vibrations within the nanoparticles. The sharp and intense peak at 1638  $\text{cm}^{-1}$  is attributed to H–O–H bending vibrations in water molecules, which also indicates the presence of moisture. Furthermore, the  $\delta\text{N-H}$  (amide II) group is confirmed by a distinct peak at 1380  $\text{cm}^{-1}$  in the biosynthesized  $\text{Co}_3\text{O}_4$  NPs [41]. Finally, the peak at 661  $\text{cm}^{-1}$  associated with the tetrahedral interaction of  $\text{Co}^{2+}$  with  $\text{O}^{2-}$  [43].

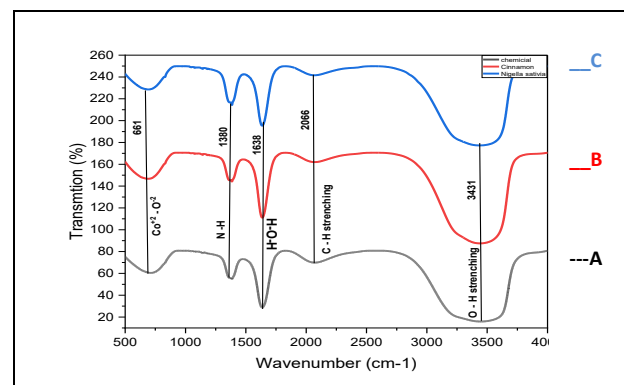


**Figure (3):** FTIR spectrum of  $\text{Co}_3\text{O}_4$  NPs with (A) Chemical method, (B) *Cinnamon* extracts (C) *Nigella sativa* extract.

## Ultraviolet-visible absorption spectra

The Ultraviolet-visible absorption spectra and the energy gap of  $\text{Co}_3\text{O}_4$  nanoparticles (NPs) synthesized with *Nigella sativa* extract, *Cinnamon* extract, and the chemical method are shown in Fig. 4. The energy gaps were calculated for the different synthesis methods using the Tauc formula [44], providing valuable insights into their optical properties. For  $\text{Co}_3\text{O}_4$  NPs made using *Nigella sativa* extract, the energy gap was found to be 1.59 eV, but the gap for the *cinnamon* extract was somewhat greater at 1.61 eV. Conversely, the  $\text{Co}_3\text{O}_4$  NPs that were chemically produced displayed a smaller energy gap of 1.43 eV [45]. These discrepancies highlight how the materials' electronic structures differ. Additionally, all three approaches yielded strong absorption edges for  $\text{Co}_3\text{O}_4$  NPs, which were compatible with the XRD data showing that the quantum confinement effect caused the energy gap to expand as nanoparticle size decreased [46]. Also, in  $\text{Co}_3\text{O}_4$  NPs made with *cinnamon* extract, an additional absorption edge and energy gap were detected at 286.8 nm. This phenomenon is explained by the existence of substances in *cinnamon*, such as cinnamaldehyde, which can interact with metals and change the constitute of nanoparticles [47, 48].

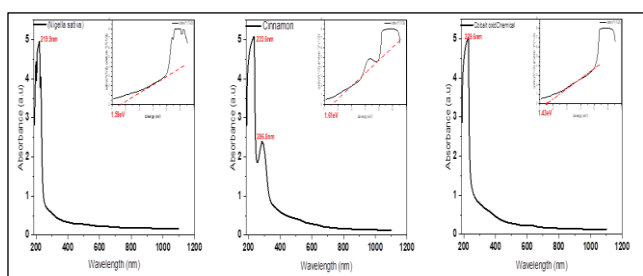


**Figure 4:** Ultraviolet-visible absorption spectra and the energy gap  $\text{Co}_3\text{O}_4$  NPs with *nigella sativa*, *cinnamon* extracts, and chemical method (left to right).

## FE-SEM and AFM

The general morphology of  $\text{Co}_3\text{O}_4$  nanostructures was analyzed using FE-SEM. As shown in Fig. 5, the nanoparticles prepared by the chemical method appeared predominantly as dot-like structures with irregular edges, uniformly distributed, having a mean particle size of about 15–35 nm [49]. The FESEM images also revealed a porous structure with voids and holes of various sizes, which increases the effective surface area of the particles. Additionally, some nanoparticles formed clusters, resulting in larger aggregated particles [49, 50]. As shown in Fig. 6, the  $\text{Co}_3\text{O}_4$  nanoparticles synthesized using *Cinnamon* extract exhibited a semi-spherical morphology, with some clustering that led to the formation of larger particles. The mean particle size for this sample ranged from 35 to 55 nm, measured using ImageJ software. Finally, as seen in Fig. 7, nanoparticles prepared with *Nigella sativa* extract displayed irregular and asymmetrical shapes, resembling uneven blocks arranged randomly. This irregular morphology is attributed to the nature of the preparation process, with a mean particle size ranging between 12.5–22.5 nm. Clusters of nanoparticles were also observed, appearing as uneven clumps.

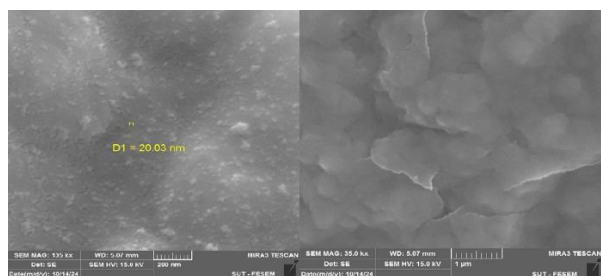


**Figure 5:** FE-SEM image of  $\text{Co}_3\text{O}_4$  NPs by Chemical method.

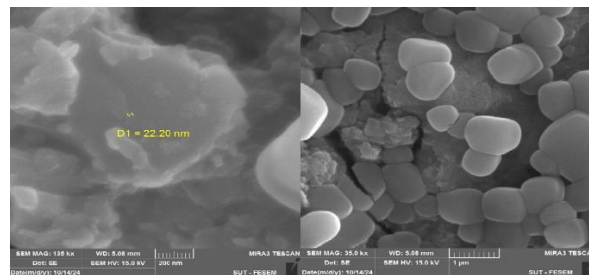


**Figure (6):** FE-SEM image of  $\text{Co}_3\text{O}_4$  NPs with *Cinnamon* extract.

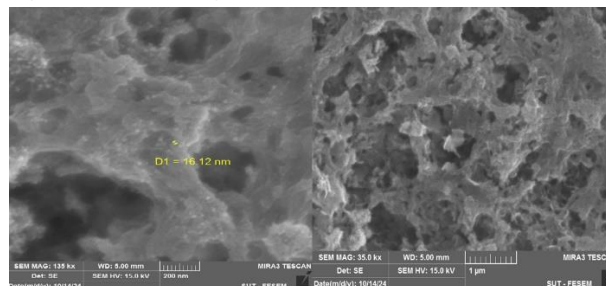


**Figure (7):** FE-SEM image of  $\text{Co}_3\text{O}_4$  NPs with *Nigella sativa* extract

The AFM analysis of  $\text{Co}_3\text{O}_4$  nanoparticles (NPs) prepared by the chemical method, as shown in Fig. 8(A), revealed a distinct nanoscale topography with a height range of up to 93.145 nm and a root mean square (RMS) roughness of 6.35 nm. The actual surface area ( $5.49 \mu\text{m}^2$ ) exceeded the projected area ( $4.00 \mu\text{m}^2$ ), reflecting an increase in effective surface area due to surface undulations. Statistical parameters, including a surface slope of 1.17 and a height distribution skewness of -0.0576, indicate slight variations with a predominance of minor depressions (51-53]. For  $\text{Co}_3\text{O}_4$  NPs prepared using *Cinnamon* extract, as seen in Fig. 8(B), the AFM analysis exposed a nanoscale topography with a height range of up to 63.39 nm. The dark regions in the image represent pits, while the light regions represent peaks, indicating surface variations with prominent peaks and deep pits. The RMS roughness was 4.48 nm, reflecting low surface roughness, which makes the surface suitable for reducing wear and friction. The actual surface area ( $4.95 \mu\text{m}^2$ ) exceeded the projected area ( $4.00 \mu\text{m}^2$ ) due to surface roughness. Statistical parameters, such as a surface slope of 0.828 and a skewness of 0.534, suggest a predominance of low surface regions with few elevated peaks [54]. In contrast, the AFM analysis of  $\text{Co}_3\text{O}_4$  NPs prepared with *Nigella sativa* extract, as shown in Fig. 8(C), revealed a maximum height of 78.1425 nm and an RMS roughness of 3.948 nm. The actual surface area ( $4.695 \mu\text{m}^2$ ) exceeded the projected area ( $4.00 \mu\text{m}^2$ ), indicating a slight increase in the interaction area due to surface undulations. Statistical parameters, including a surface slope of 0.724 and a skewness of 0.1046, suggest a predominance of minor depressions and scattered sharp peaks. High kurtosis values indicated low to moderate surface roughness with scattered sharp features. The topographical distribution showed overall smoothness with a tilt in a specific direction ( $162.39^\circ$ ), possibly due to the manufacturing process or thermal treatment. The low roughness and positive skewness values suggest that most of the terrain consists of elevated peaks rather than deep depressions.

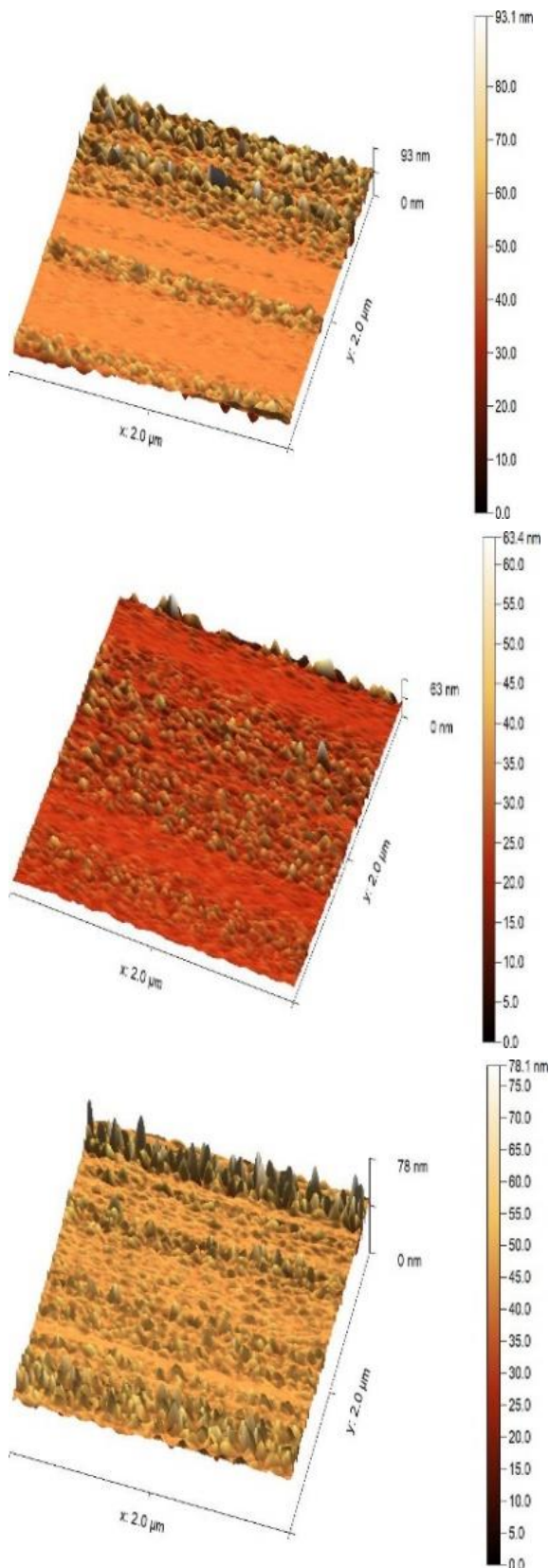


**Figure (8):** Atomic Force Microscopy of  $\text{Co}_3\text{O}_4$  NPs with chemical method, Cinnamon extracts, and *Nigella sativa* (Left to right).

**Table (2):** Effect of  $\text{Co}_3\text{O}_4$  NPs with additives on bacterial growth.

Bacteria model	Cinnamon	Chemical	<i>Nigella sativa</i>
<i>Staphylococcus aureus</i>	34	33	32
<i>Staphylococcus epidermidis</i>	34	34	33
<i>Escherichia coli</i>	30	29	28
<i>Klebsiella sp</i>	31	34	32
<i>Candida albicans</i>	40	36	41

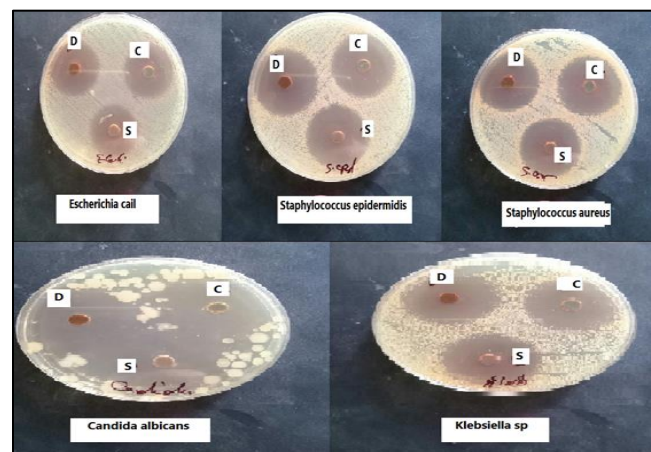


**Figure (9):** Antimicrobial activity of  $\text{Co}_3\text{O}_4$  NPs synthesized by (D) Cinnamon extract; (C) Chemical Method; (S) *Nigella sativa*.

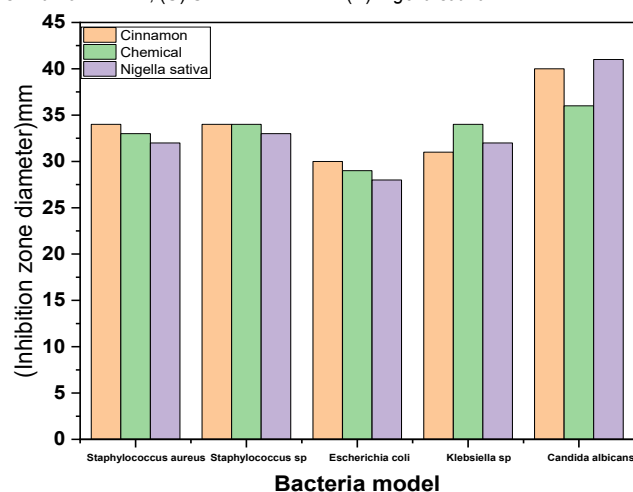


**Figure (10):** Effect of  $\text{Co}_3\text{O}_4$  NPs with additives on bacterial growth.

### Antibacterial Activity

Fig. 9 and Fig.10 illustrate the effects of three cobalt oxide nanoparticle ( $\text{Co}_3\text{O}_4$  NP) samples, synthesized using plant extracts and the chemical method, on various types of bacteria and fungi. The data in Table 2, expressed as the range of the inhibition zone in millimeters surrounding the samples placed on Mueller-Hinton agar plates, reflect the antimicrobial activity of each sample. The size of the inhibition zone indicates the sample's effectiveness in inhibiting or killing microbial growth. The sample containing  $\text{Co}_3\text{O}_4$  NPs with Cinnamon extract demonstrated significant effectiveness against *Staphylococcus aureus* (34 mm) and *Escherichia coli* (30 mm). This result is attributed to the presence of cinnamaldehyde, an essential oil compound with potent antibacterial properties. The synergy between cobalt oxide and cinnamaldehyde enhanced the antibacterial efficacy against Gram-positive (*S. aureus*) and Gram-negative (*E. coli*).  $\text{Co}_3\text{O}_4$  NPs synthesized via the chemical method showed robust results, particularly against *Klebsiella sp.* (34 mm), and exhibited balanced performance against other microbes. This is likely due to the small, homogeneous particle size, which increases the active surface area and facilitates the penetration of the outer layer of Gram-negative bacteria like *Klebsiella sp.*, which are typically more resistant. Chemically synthesized nanoparticles generate a substantial amount of free oxygen radicals, such as hydroxyl radicals ( $\cdot\text{OH}$ ), superoxide anions ( $\text{O}_2^-$ ), and hydrogen peroxide ( $\text{H}_2\text{O}_2$ ). These radicals disrupt the outer layer of Gram-negative bacteria, damaging their DNA and proteins, ultimately leading to cell death. When  $\text{Co}_3\text{O}_4$  NPs are combined with natural additives like cinnamaldehyde (from Cinnamon) or thymoquinone (from *Nigella sativa*), the production of free radicals may decrease due

to interactions between cobalt and the natural compounds. This can reduce the direct antimicrobial activity, as the concentration of active substances influences bacterial resistance. Some compounds in natural extracts may interact with cobalt oxide, partially inhibiting its direct activity. For instance, Gram-negative *Klebsiella sp.* may exhibit increased resistance to natural additives, whereas chemically synthesized  $\text{Co}_3\text{O}_4$  NPs retain a strong ability to penetrate bacterial membranes and interact with intracellular components. *Nigella sativa*-based  $\text{Co}_3\text{O}_4$  NPs displayed the highest effectiveness against *Candida albicans* (41 mm). This exceptional antifungal activity is attributed to thymoquinone, a potent antifungal compound that disrupts fungal cell walls, inhibits metabolic activity, and enhances the inhibitory effect through synergy with cobalt oxide. For Gram-positive bacteria like *S. aureus*, the thick peptidoglycan wall increases susceptibility to antimicrobial agents like cinnamaldehyde. Gram-negative bacteria (*Klebsiella sp.* and *E. coli*), with their additional outer membrane, exhibit greater resistance. However,  $\text{Co}_3\text{O}_4$  NPs, especially when combined with active substances, effectively penetrate this barrier. The strong response of *Candida albicans* to *Nigella sativa* emphasizes the direct impact of thymoquinone on fungal cell walls and highlights the antifungal potency of this combination.

## Conclusion

Several conclusions were drawn from the synthesis and examination of nanoparticles of cobalt oxide ( $\text{Co}_3\text{O}_4$  NPs). Firstly,  $\text{Co}_3\text{O}_4$  NPs were effectively created via a green synthesis technique that is both economical and ecologically benign, utilizing extracts from *Cinnamomum zeylanicum* (Cinnamon) and *Nigella sativa*. For comparison,  $\text{Co}_3\text{O}_4$  NPs were also prepared using conventional chemical synthesis. The nanoparticles were examined with various approaches, such as using various techniques, including FTIR, XRD, FESEM, AFM, and UV-Vis spectroscopy, all of which confirmed effective fabrication of  $\text{Co}_3\text{O}_4$  NPs. The average crystalline size and band gap energy were found to be 5.49 nm and 1.61 eV for Cinnamon-assisted NPs, 7.22 nm and 1.59 eV for *Nigella sativa*-assisted NPs, and 10.6 nm and 1.43 eV for chemically synthesized NPs. These results indicate an improvement in the electronic structure and a pronounced quantum confinement effect as particle size decreases. FTIR analysis revealed active chemical groups such as N-H, C-H, and O-H, confirming the role of plant extracts in enhancing chemical reactions and introducing functional properties to the nanoparticles. FESEM analysis demonstrated that nanoparticles synthesized with plant extracts exhibited irregular shapes and smaller sizes, leading to an increased effective surface area. This increased surface area enhanced the biological activity of the nanoparticles against bacteria and fungi. AFM analysis further confirmed distinct surface topographies for the plant-assisted NPs, including reduced surface roughness for Cinnamon-assisted NPs and increased height variations. The antimicrobial activity of  $\text{Co}_3\text{O}_4$  NPs synthesized with natural extracts surpassed that of the chemically synthesized NPs. *Cinnamon* and *Nigella sativa* extracts exhibited significant effectiveness against both Gram-negative and Gram-positive bacteria, as well as the fungus *Candida albicans*. This superior performance is attributed to the interaction between active compounds like cinnamaldehyde (in *Cinnamon*) and thymoquinone (in *Nigella sativa*) with the nanoparticles, enhancing their membrane penetration and reactivity. In conclusion, the use of plant extracts not only facilitates the fabrication of  $\text{Co}_3\text{O}_4$  nanoparticles with reduced crystallite dimensions and improved energy gaps but also provides an eco-friendly and sustainable substitute for chemical techniques. This green synthesis approach holds significant

potential for expanding the applications of nanoparticles in various domains, including industry, energy, and medicine.

## Disclosure Statement

- **Ethics approval:** Not applicable
- **Consent for publication:** Not applicable
- **Availability of data and materials:** The raw data required to reproduce these findings are available in the body and illustrations of this manuscript.
- **Author's contribution:** Study conception and design: Ghasaq Z. Alwan, Raed Jumah Almansouri; theoretical calculations and modeling: Hana H. Kareem, Emtinan Mohammed Jawad; data analysis and validation: Ghasaq Z. Alwan. Draft manuscript preparation: Emtinan Mohammed Jawad, Raed Jumah Almansouri. All authors reviewed the results and approved the final version of the manuscript.
- **Funding:** None.
- **Conflicts of interest:** The authors declare that there is no conflict of interest regarding the publication of this article
- **Acknowledgements:** The authors thank Mustansiriyah University, Baghdad, Iraq, for supporting the presented work.

## Open Access

This article is licensed under a Creative Commons Attribution 4.0 International License, which permits use, sharing, adaptation, distribution and reproduction in any medium or format, as long as you give appropriate credit to the original author(s) and the source, provide a link to the Creative Commons licence, and indicate if changes were made. The images or other third party material in this article are included in the article's Creative Commons licence, unless indicated otherwise in a credit line to the material. If material is not included in the article's Creative Commons licence and your intended use is not permitted by statutory regulation or exceeds the permitted use, you will need to obtain permission directly from the copyright holder. To view a copy of this license, visit <https://creativecommons.org/licenses/by-nc/4.0/>

## References

- 1] El-Shafie AS, Ahsan I, Radhwani M, Al-Khang MA, El-Azazy M. Synthesis and Application of Cobalt Oxide ( $\text{Co}_3\text{O}_4$ )-Impregnated Olive Stones Biochar for the Removal of Rifampicin and Tigecycline: Multivariate Controlled Performance. *Nanomaterials*. 2022;12(3):379.
- 2] Aziz WJ, Alwan GZ, Sabry RS. Evaluation the effect of the difference of plant extract (oats) from animal extract (chitosan) on the properties of chromium oxide NPs. *AIP Conference Proceedings*. 2024;2922(1).
- 3] Salameh S, Soboh S, Bsharat A, Maali R, Assali M, Ishtaiwi M, et al. Preparation of Silver Nanoparticles/Polyvinyl alcohol Nanocomposite Films with Enhanced Electrical, Thermal, and Antimicrobial Properties. *An-Najah University Journal for Research - A (Natural Sciences)* [Internet]. 2025 Feb;39(3). Available from: <http://dx.doi.org/10.35552/aujr.a.39.3.2380>.
- 4] Alabi MA, Oladoye EO, Adedokun TA, Adebisi AA, Olatoye RS, Ajani BK, et al. Exploring the Therapeutic Potential of *Antiaris africana*: Targeting Cyclin-Dependent Kinases 8 and 13 for Cancer Treatment through Molecular Docking Studies. *Al-Mustansiriyah Journal of Science*. 2025;36(2):41-58.

- 5] Hawkey PM. The growing burden of antimicrobial resistance. *Journal of Antimicrobial Chemotherapy*. 2008;62(suppl\_1):i1-i9.
- 6] Lowy FD. *Staphylococcus aureus* infections. *New England Journal of Medicine*. 1998;339(8):520-32.
- 7] Dadi R, Azouani R, Traore M, Mielcarek C, Kanaev A. Antibacterial activity of ZnO and CuO nanoparticles against gram positive and gram negative strains. *Materials Science and Engineering: C*. 2019;104:109968.
- 8] Rosi NL, Mirkin CA. Nanostructures in Biodiagnostics. *Chemical Reviews*. 2005;105(4):1547-62.
- 9] Xiang Y, Li J, Liu X, Cui Z, Yang X, Yeung KWK, et al. Construction of poly(lactic-co-glycolic acid)/ZnO nanorods/Ag nanoparticles hybrid coating on Ti implants for enhanced antibacterial activity and biocompatibility. *Materials Science and Engineering: C*. 2017;79:629-37.
- 10] Gold K, Slay B, Knackstedt M, Gaharwar AK. Antimicrobial Activity of Metal and Metal-Oxide Based Nanoparticles. *Advanced Therapeutics*. 2018;1(3):1700033.
- 11] Bailey DM, Davies B. Acute Mountain Sickness; Prophylactic Benefits of Antioxidant Vitamin Supplementation at High Altitude. *High Altitude Medicine & Biology*. 2001;2(1):21-9.
- 12] Podsędek A. Natural antioxidants and antioxidant capacity of Brassica vegetables: A review. *LWT - Food Science and Technology*. 2007;40(1):1-11.
- 13] Shakir MS, Khosa MK, Zia KM, Saeed M, Bokhari TH, Zia MA. Investigation of thermal, antibacterial, antioxidant and antibiofilm properties of PVC/ABS/ZnO nanocomposites for biomedical applications. *Korean Journal of Chemical Engineering*. 2021;38(11):2341-6.
- 14] Abdullah AM, Attia AJK, Shtykov SN. Synthesis and Characterization of Novel Benzimidazole Derivatives using CdO NPs and their Application as Antibacterial and Antifungal Agents. *Al-Mustansiriyah Journal of Science*. 2024;35(4):52-63.
- 15] Uma Suganya KS, Govindaraju K, Ganesh Kumar V, Stalin Dhas T, Karthick V, Singaravelu G, et al. Blue green alga mediated synthesis of gold nanoparticles and its antibacterial efficacy against Gram positive organisms. *Materials Science and Engineering: C*. 2015;47:351-6.
- 16] Reddy NJ, Nagoor Vali D, Rani M, Rani SS. Evaluation of antioxidant, antibacterial and cytotoxic effects of green synthesized silver nanoparticles by Piper longum fruit. *Materials Science and Engineering: C*. 2014;34:115-22.
- 17] Bao Y, Krishnan KM. Preparation of functionalized and gold-coated cobalt nanocrystals for biomedical applications. *Journal of Magnetism and Magnetic Materials*. 2005;293(1):15-9.
- 18] Singh DM, Singh S, Prasad S, Gambhir I. Nanotechnology in medicine and antibacterial effect of silver nanoparticles. *Digest Journal of Nanomaterials and Biostructures*. 2008;3:115-22.
- 19] Khanna PK, Singh N, Charan S, Subbarao VVVS, Gokhale R, Mulik UP. Synthesis and characterization of Ag/PVA nanocomposite by chemical reduction method. *Materials Chemistry and Physics*. 2005;93(1):117-21.
- 20] Chandran SP, Chaudhary M, Pasricha R, Ahmad A, Sastry M. Synthesis of Gold Nanotriangles and Silver Nanoparticles Using Aloe Vera Plant Extract. *Biotechnology Progress*. 2006;22(2):577-83.
- 21] Lee SY, Krishnamurthy S, Cho C-W, Yun Y-S. Biosynthesis of Gold Nanoparticles Using *Ocimum sanctum* Extracts by Solvents with Different Polarity. *ACS Sustainable Chemistry & Engineering*. 2016;4(5):2651-9.
- 22] Iravani S. Green synthesis of metal nanoparticles using plants. *Green Chemistry*. 2011;13(10):2638-50.
- 23] Schröfel A, Kratošová G, Šafařík I, Šafaříková M, Raška I, Šor LM. Applications of biosynthesized metallic nanoparticles – A review. *Acta Biomaterialia*. 2014;10(10):4023-42.
- 24] Das RK, Golder AK. Co<sub>3</sub>O<sub>4</sub> spinel nanoparticles decorated graphite electrode: Bio-mediated synthesis and electrochemical H<sub>2</sub>O<sub>2</sub> sensing. *Electrochimica Acta*. 2017;251:415-26.
- 25] Salam MA, AbuKhadra MR, Mohamed AS. Effective oxidation of methyl parathion pesticide in water over recycled glass based-MCM-41 decorated by green Co<sub>3</sub>O<sub>4</sub> nanoparticles. *Environmental Pollution*. 2020;259:113874.
- 26] Mittal AK, Chisti Y, Banerjee UC. Synthesis of metallic nanoparticles using plant extracts. *Biotechnology Advances*. 2013;31(2):346-56.
- 27] Hassan MA, Hassan NA, Khalaf SK. Electron Microscope Scanning, and Antibacterial Activity of TiO<sub>2</sub> Nanoparticles on pathogenic strains of *Staphylococcus aureus* and *Escherichia coli*. *Diyala Journal of Medicine*. 2024 Apr 25;26(1):79-91.
- 28] Alaghemand A, Khaghani S, Bihamta MR, Gomarian M, Ghorbanpour M. Green Synthesis of Zinc Oxide Nanoparticles Using *Nigella Sativa* L. Extract: The Effect on the Height and Number of Branches. *Journal of Nanostructures*. 2018;8(1):82-8.
- 29] Yan D, Zhao H, Liu Y, Wu X, Pei J. Shape-controlled synthesis of cobalt particles by a surfactant-free solvothermal method and their catalytic application to the thermal decomposition of ammonium perchlorate. *CrystEngComm*. 2015;17(47):9062-9.
- 30] Abu-Zied BM, Alamry KA. Green synthesis of 3D hierarchical nanostructured Co<sub>3</sub>O<sub>4</sub>/carbon catalysts for the application in sodium borohydride hydrolysis. *Journal of Alloys and Compounds*. 2019;798:820-31.
- 31] Dubey S, Kumar J, Kumar A, Sharma YC. Facile and green synthesis of highly dispersed cobalt oxide (Co<sub>3</sub>O<sub>4</sub>) nano powder: Characterization and screening of its eco-toxicity. *Advanced Powder Technology*. 2018;29(11):2583-90.
- 32] Bibi I, Nazar N, Iqbal M, Kamal S, Nawaz H, Nouren S, et al. Green and eco-friendly synthesis of cobalt-oxide nanoparticle: Characterization and photo-catalytic activity. *Advanced Powder Technology*. 2017;28(9):2035-43.
- 33] Akhlaghi N, Najafpour-Darzi G, Younesi H. Facile and green synthesis of cobalt oxide nanoparticles using ethanolic extract of *Trigonella foenum-graecum* (Fenugreek) leaves. *Advanced Powder Technology*. 2020;31(8):3562-9.
- 34] Saeed SY, Mazhar K, Raees L, Mukhtiar A, Khan F, Khan M. Green synthesis of cobalt oxide nanoparticles using roots extract of *Ziziphus Oxyphylla* Edgew its characterization and antibacterial activity. *Materials Research Express*. 2022;9(10):105001.
- 35] Anjum S, Jacob G, Gupta B. Investigation of the herbal synthesis of silver nanoparticles using Cinnamon zeylanicum extract. *Emergent Materials*. 2019;2(1):113-22.
- 36] Saxena R, Kotnala S, Bhatt SC, Uniyal M, Rawat BS, Negi P, Riyal MK. A review on green synthesis of nanoparticles toward sustainable environment. *Sustainable Chemistry for Climate Action*. 2025 Apr 16:100071.

- 37] Mubraiz N, Bano A, Mahmood T, Khan N. Microbial and Plant Assisted Synthesis of Cobalt Oxide Nanoparticles and Their Antimicrobial Activities. *Agronomy*. 2021;11(8):1607.
- 38] Singh AK. A review on plant extract-based route for synthesis of cobalt nanoparticles: Photocatalytic, electrochemical sensing and antibacterial applications. *Current Research in Green and Sustainable Chemistry*. 2022;5:100270.
- 39] Monica Ahmad N, Husaini Mohamed A, Hasan NA, Zainal-Abidin N, Zaini Nawahwi M, Mohamad Azzeme A. Effect of optimisation variable and the role of plant extract in the synthesis of nanoparticles using plant-mediated synthesis approaches. *Inorganic Chemistry Communications*. 2024;161:111839.
- 40] Chatterjee AK. 8 - X-Ray Diffraction. In: Ramachandran VS, Beaudoin JJ, editors. *Handbook of Analytical Techniques in Concrete Science and Technology*. Norwich, NY: William Andrew Publishing; 2001. p. 275-332.
- 41] Karse SD, Fite MC. Studies on structural and optical properties of cobalt oxide nanoparticles using co-precipitation. *Physica B: Condensed Matter*. 2024;689:416181.
- 42] Salavati-Niasari M, Khansari A, Davar F. Synthesis and characterization of cobalt oxide nanoparticles by thermal treatment process. *Inorganica Chimica Acta*. 2009;362(14):4937-42.
- 43] Karvekar OS, Vadanagekar AS, Sarvalkar PD, Suryawanshi SS, Jadhav SM, Singhan RD, et al. Bos taurus (A-2) urine assisted bioactive cobalt oxide anchored ZnO: a novel nanoscale approach. *Scientific Reports*. 2022;12(1):15584.
- 44] Jubu PR, Danladi E, Ndeze UI, Adedokun O, Landi S, Haider AJ, et al. Comment about the use of unconventional Tauc plots for bandgap energy determination of semiconductors using UV-Vis spectroscopy. *Results in Optics*. 2024;14:100606.
- 45] Albakry Z, Karrar E, Mohamed Ahmed IA, Ali AA, Al-Maqtari QA, Zhang H, et al. A comparative study of black cummin seed (*Nigella sativa* L.) oils extracted with supercritical fluids and conventional extraction methods. *Journal of Food Measurement and Characterization*. 2023;17(3):2429-41.
- 46] Hafedh FR, Mohammed HH, Mageed ZN. Synthesis and Characterization of Novel Pyrimido [1,2-a] benzimidazole and its Derivatives. *Al-Mustansiriyah Journal of Science*. 2022;33(1):15-20.
- 47] Salim AA, Ghoshal SK, Suan LP, Bidin N, Hamzah K, Duralim M, et al. Liquid media regulated growth of cinnamon nanoparticles: Absorption and emission traits. *Malaysian Journal of Fundamental and Applied Sciences*. 2018;14(3-1):447-9.
- 48] Pagar T, Ghotekar S, Pagar K, Pansambal S, Oza R. A Review on Bio-Synthesized Co<sub>3</sub>O<sub>4</sub> Nanoparticles Using Plant Extracts and their Diverse Applications. *Journal of Chemical Reviews*. 2019;1(4):260-70.
- 49] Pinalia A, Yulizar Y, Wibowo HB, Apriandanu DOB. Co<sub>3</sub>O<sub>4</sub> nanoparticles: Facile preparation, characterization and their catalytic activity towards thermal decomposition of ammonium perchlorate. *AIP Conference Proceedings*. 2020;2226(1).
- 50] Farahmandjou M, Shadrokh S. Preparation of Ferromagnetic Co<sub>3</sub>O<sub>4</sub> Nanoparticles by Wet Chemical Synthesis Method. *To Physics Journal*. 2019;3:89-99.
- 51] Hassan MA. Histological Determination of Cinnamon and Olive Oil Extract on Traumatic Oral Ulcer in Laboratory Rabbit. *Diyala Journal of Medicine*. 2024 Oct 25;27(1):111-22.
- 52] Jabbar KK, Bouaziz M. Antioxidant and Anticancer Activities of Silver Nanoparticles Synthesized Using Cinnamon Extracts. *Al-Mustansiriyah Journal of Science*. 2025;36(2):18-29.
- 53] Nasif HK, Ahmed BM, Aadim KA. Synthesis Emission Spectra of (LIPS) Technique for Cu, Ag Nanoparticles and their Antibacterial Activity. *Al-Mustansiriyah Journal of Science*. 2021;32(3):49-57.
- 54] David SA, Veeraputhiran V, Vedhi C. Biosynthesis of cobalt oxide nanoparticles-a short review. *Journal of Nanoscience and Technology*. 2019:734-7.